

Excited State Proton Transfers and Subsequent Electron Rearrangement of Aqueous 6-Hydroxyquinoline

Hyunung Yu, Hyuk-Jin Kwon, and Du-Jeon Jang*[†]

Department of Chemistry, Seoul National University, Seoul 151-742, Korea

Received October 10, 1996

Aqueous 6-hydroxyquinoline in the first excited singlet state undergoes protonation to the imine group first in 15 ps, then in the time scale of 40 ps deprotonation from the enol group and finally, however, quickly as in 11 ps electron rearrangement to change into a resonance hybrid structure of quinoid-prevailing forms. Despite the fact that the decay time constant is smaller than the formation time constant, fluorescence from excited prototropic zwitterion is observed to assign its maximum at 510 nm. The electron rearrangement is basically an intramolecular charge transfer from the deprotonated oxygen atom to the positively charged iminium ring without any notable change in nuclear geometry, producing a zwitterionic quinoid structure with much a smaller electric dipole moment than the zwitterionic prototropic species. This photoproduct formed by consecutive excited state proton and electron transfers shows a smaller dipole moment in S_1 than in S_0 and a hypsochromic shift although its S_1 state has (π, π^*) character.

Introduction

Important photochemical consequences of the changes in molecular structure and electronic distribution which occur upon electronic excitation are the qualitative and quantitative changes of chemical properties at excited states. It is well known¹ that the character of S_1 (π, π^*) state is zwitterionic and concerted while that of S_1 (n, π^*) state is diradicaloid and unconcerted. Various molecular species are known to undergo acid-base reaction,²⁻⁶ charge transfer,⁷⁻¹¹ hydrogen abstraction¹²⁻¹⁵ or electron abstraction¹⁶ in their first excited singlet states before electronic deactivation to their ground states. Considering the characteristic natures of S_1 states, we can understand the reasons that a molecule in S_1 (π, π^*) state often undergoes proton or electron transfer reaction concertedly, while a molecule in S_1 (n, π^*) state goes through hydrogen atom or electron abstraction reaction.

Proton and charge transfer reactions are ubiquitous and very important in many chemical and biological processes. Charge transfer reaction is one of the most attractive fields of chemical study, since it does not only include proton transfers but also describe most chemical reactions such as photoinduced electron transfer, dynamics for the formation and decay of radical ion pairs and dissociative electron transfer. Photoinduced proton and charge transfer reactions in organic, inorganic and biological molecular systems have been extensively studied recently using various time-resolved laser spectroscopic techniques¹⁷⁻²¹ since the investigations not only provide us the vivid pictures of photoinduced transfer processes but also facilitate to understand the relations of various different properties to one another systematically.

Hydroxyquinolines and their derivatives are very interesting species in both fundamental and practical aspects. 8-Hydroxyquinoline and its derivatives have been used as analytical reagents for the spectrophotometric determination of metal ions²² and chelating ion-exchangers²³ and photonic devices such as LED,²⁴ semiconductor²⁵ and electroluminescence²⁶ since they exhibit unique complexing and fluo-

rogenic properties. 7-Hydroxyquinoline and its derivatives provide a model for understanding photoinduced relay or concerted proton transfer cycles in various environments.²⁷⁻³¹ 6-Hydroxyquinoline (6HQ) shows photoinduced coupled proton and electron transfers³² while 5-hydroxyquinoline derivative is employed as adhesives in forest products industry.³³ 4-Hydroxyquinoline derivatives are applied as antibacterial drugs, dehydrogenase inhibitors or reductase inhibitors^{34,35} and 3-hydroxyquinoline derivatives as excited state proton transfer³⁶ and antibiotic reagents.^{37,38} Studies^{39,40} on the intramolecular hydrogen bonding and organometallic complexing properties of 2-hydroxyquinoline are also interesting.

Since one hydroxyquinoline molecule has two prototropic functional groups, four prototropic species of normal molecule (HQ), enol-deprotonated anion ($^-$ QN), imine-protonated cation (HQNH $^+$) and enol-deprotonated and imine-protonated zwitterion ($^-$ QNH $^+$) are equilibrated in aqueous hydroxyquinoline solutions as drawn in Figure 1. The enol and imine groups of 3-, 6- and 7-hydroxyquinolines become more acidic and basic respectively in the first excited singlet state than in the ground state.³⁶ As a result of these pK differences, the deprotonation of enol group and the protonation of imine group in S_1 and their reverse processes in T_1 and S_0 are extensively studied.²⁷⁻³² In addition to these prototropic changes, intramolecular electron transfer is also reported in the first excited singlet states of 6HQ prototropic species.³²

This paper presents our study on the excited state proton transfer and subsequent electron rearrangement reactions of aqueous 6HQ solutions by measuring picosecond time-resolved fluorescence kinetic profiles as well as static absorption and emission spectra. This work does not only report the formation and decay times and peak fluorescence wavelengths of individual species but also manifest a complete mechanism of proton and electron transfer reactions in the first excited singlet states of aqueous 6HQ prototropic and electropic species.

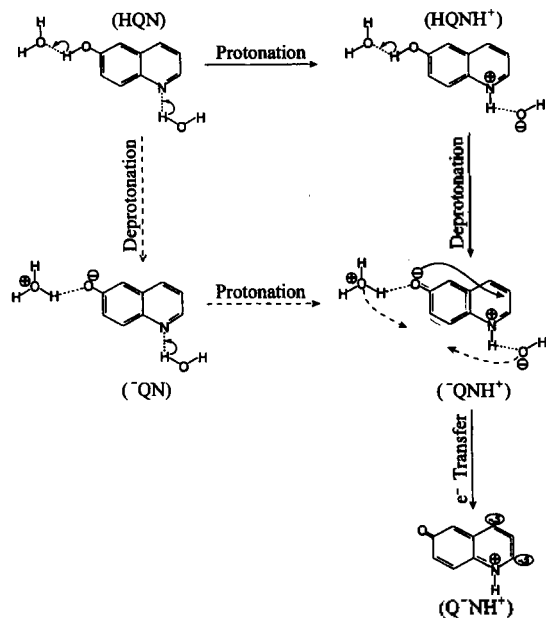


Figure 1. Scheme illustrating the excited state proton and electron transfer mechanism of aqueous 6HQ neutral solution. Protonation to the imine group takes place first, forming HQNH⁺ as the reaction intermediate in the course of protropic tautomerization. -QNH⁺ generated by the subsequent deprotonation of the enol group is transformed into a resonance hybrid structure of quinoid-dominant forms by an intramolecular electron transfer from the deprotonated oxygen atom to the iminium ring.

Experimental

Aqueous solutions were prepared simply by dissolving vacuum-sublimed 98% 6HQ, purchased from the Aldrich, in distilled water. These aqueous solutions will be called as neutral solutions to be distinguished from extremely acidic or basic solutions, although the measured pHs of these solutions were actually lower than 7, probably owing to dissolved CO₂. Nonneutral solutions were prepared by dissolving sublimed 6HQ in aqueous solutions of given HClO₄ or NaOH concentrations. Typical 6HQ concentration was 0.2 mM. All the experiments were done at room temperature and the results presented hereafter were obtained from undegassed, unbuffered, neutral and aqueous 6HQ solutions if not specifically indicated otherwise.

Samples in emission measurements were excited by a wavelength-selected beam from a 350-W Xe lamp (Schoeffel, LPS 255 HR) using a 0.275-m monochromator (ARC, Spectrapro-275). Luminescence was collected from the front surface of sample excitation and focused to a 0.25-m monochromator (Kratos, GM 252) which was attached with a photomultiplier tube (Hamamatsu, R374). Emission spectra reported here were not corrected for the wavelength-dependent variation of detector sensitivity. Absorption spectra were measured using a homemade spectrometer which was assembled with a W/H₂ lamp and a 0.25-m monochromator (Kratos, GM 252).

Picosecond time-resolved fluorescence kinetic profiles were measured using a previously described⁴¹ time-correlated single photon counting system of a 70-ps-fwhm response time equipped with a Coherent Antares YAG-

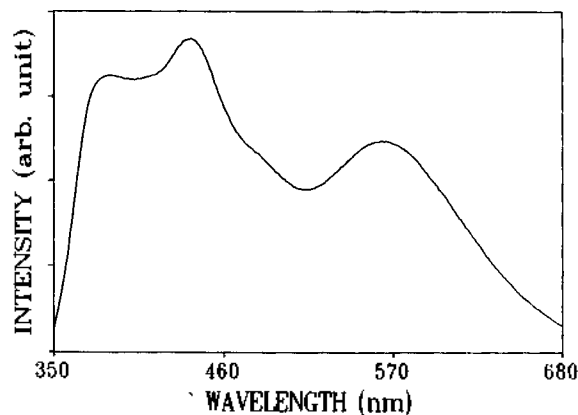


Figure 2. Emission spectrum, excited at 325 nm, of 0.2-mM 6HQ aqueous solution.

pumped, hybrid mode-locked and cavity-dumped dye laser. Samples were excited only by frequency-doubled R6G dye laser pulses of 290 nm because of limited laser availability. Fluorescence collected from the front surface of sample excitation was dispersed by a 0.2-m Jobin-Yvon spectrometer and then focused into a Hamamatsu R2809-07 MCP. The signal from the MCP was used to stop a time-to-amplitude converter (Ortec 457) already started by a fast photodiode. Fluorescence time constants were deconvoluted using a relative non-linear least squares method.

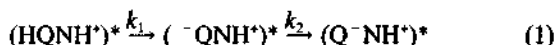
Results and Discussion

When 6HQ aqueous solution was excited at 325 nm, the peak absorption wavelength of the lowest HQN electronic transition, the emission spectrum shows three distinguishable peaks at least as given in Figure 2. The emission band with the peak near 440 nm is emitted from excited HQNH⁺ which is produced by protonation to the imine group of HQN upon absorption of a photon while the emission with the peak at 380 nm is normal fluorescence from excited HQN species. The emission band with the peak at 560 nm arises from an excited resonance hybrid structure of quinoid-dominant forms (Q-NH⁺)* which is transformed from (-QNH⁺)* by electron rearrangement, as reported by Bardez *et al.*³² No appearance of an emission peak accountable to excited -QNH⁺ indicates that (-QNH⁺)* is not stable, unlike the excited zwitterionic species of 7-hydroxyquinoline which is the final photoproduct in S₁ with a long lifetime of 3 ns.²⁹

The results of fluorescence kinetic studies given in Figure 3 and Table 1 indicate that the reaction pathway in S₁, inferred from static fluorescence results, is correct. Since five kinds of protropic and electropic species are possible to exist in S₁ only, very careful analyses were necessary to obtain the rise and decay time constants of fluorescence as well as the wavelengths of peak fluorescence for respective species. Since an organic fluorescence band is broad and has a long red tail, a fluorescence kinetic profile at a certain wavelength usually contains the formation and decay kinetics of more than one species so that apparent fluorescence time constants do not point out directly the deconvoluted formation and decay times of respective species involved in

sequential reactions. Figure 3 shows that both the formation and decay times increase as the monitoring fluorescence wavelength increases. These as a whole indicate that the species emitting higher energy light sequentially transforms in S_1 into the one emitting lower energy light. The kinetic profiles at 370 and 430 nm show a very slowly decaying component also, which we think originates from excited impurity species that are neither 6HQN nor its photoinduced protropic species.

As illustrated in Figure 1, upon absorption of a photon aqueous HQN species in neutral solution undergoes protonation to the imine group first in 15 ps, then deprotonation from the enol group in 40 ps and finally but immediately intramolecular charge transfer from the deprotonated oxygen atom to the positively charged iminium ring in 11 ps, producing the zwitterionic quinoid structure as the final photochemical product in S_1 . The charge transfer time of 11 ps was calculated from the difference between the decay time of $(^-\text{QNH}^+)^*$ fluorescence and the rise time of $(\text{Q}^-\text{NH}^+)^*$ fluorescence as follows.



$$[(\text{HQN}^+)^*]_0 = [(\text{HQN}^+)^*] + [(^-\text{QNH}^+)^*] + [(\text{Q}^-\text{NH}^+)^*] \quad (2)$$

Assuming the downward relaxation rates of $(\text{HQN}^+)^*$ and $(^-\text{QNH}^+)^*$ are negligible compared with the respective photochemical reaction rates so that the $(k_1)^{-1}$ and $(k_2)^{-1}$ are the same as the respective fluorescence lifetimes of $(\text{HQN}^+)^*$

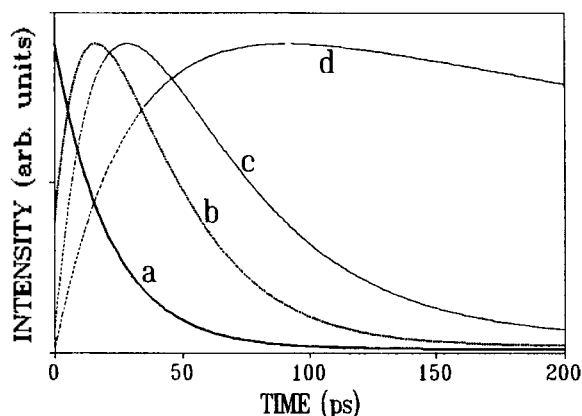


Figure 3. Instrumental response function-deconvoluted fluorescence kinetic profiles of 0.2-mM 6HQN aqueous solution, excited at 290 nm and monitored at 370 (a), 430 (b), 490 (c) and 580 nm (d), respectively.

and $(^-\text{QNH}^+)^*$ and assuming the condition of Eq. (2), we can express the time-dependent concentration of $(\text{Q}^-\text{NH}^+)^*$ as Eq. (3)

$$[(\text{Q}^-\text{NH}^+)^*] = \left\{ 1 + \frac{k_1 e^{-k_2 t} - k_2 e^{-k_1 t}}{k_2 - k_1} \right\} [(\text{HQN}^+)^*]_0 \quad (3)$$

and correlate this with its measured time-dependent concentration formation of Eq. (4).

$$[(\text{Q}^-\text{NH}^+)^*] = (1 - e^{-k_1 t}) [(\text{HQN}^+)^*]_0 \quad (4)$$

Since $k_1 = (40 \text{ ps})^{-1}$ and $k_2 = (30 \text{ ps})^{-1}$, we can find that the intramolecular charge transfer rate of k_2 is $(11 \text{ ps})^{-1}$. We can also estimate with the values of k_1 and k_2 that the fraction of $(^-\text{QNH}^+)^*$ fluorescence to $(\text{HQN}^+)^*$ fluorescence is about 23%, assuming that the Einstein's spontaneous emission coefficients of both the species are the same except the variations owing to ν^3 dependence. The contribution of $(^-\text{QNH}^+)^*$ fluorescence might be noticed by observing the weak shoulder near 480 nm in Figure 2. Our observation of $(^-\text{QNH}^+)^*$ fluorescence is contrasting with the previous assertion³² that $(^-\text{QNH}^+)^*$ species is not fluorescent.

Table 1 also exhibits that $(\text{HQN}^+)^*$ in 4-M HClO_4 aqueous solution undergoes enol deprotonation in 960 ps and immediately subsequent electron rearrangement in 26 ps while $(^-\text{QN})^*$ in 1-M NaOH aqueous solution goes through imine protonation in 15 ps and is subject to the subsequent electron transfer in 48 ps. The extremely fast imine protonation time of 15 ps in the strongly basic solution and the contrastively slow enol deprotonation time of 960 ps in the strongly acidic solution confirm the photochemical pathway given in Figure 1 that $(\text{HQN}^+)^*$ species, brought to birth first by the imine protonation of $(\text{HQN})^*$, is the protropic reaction intermediate in S_1 , which experiences enol deprotonation in a slower time scale. It is interesting to note that upon absorption of a photon aqueous 7-hydroxyquinoline normal species transforms into both $(\text{HQN}^+)^*$ and $(^-\text{QN})^*$ as the protropic reaction intermediates in S_1 .²⁹ The imine protonation and enol deprotonation processes at S_1 are sequential in 6HQN neutral aqueous solution while they are competitive in 7-hydroxyquinoline one.

The intramolecular electron transfer process in neutral solution, portrayed in the later part of Figure 1, becomes slower in acidic solution and slowest in basic solution. Since the electron transfer from the deprotonated oxygen atom to the iminium ring of $(^-\text{QNH}^+)^*$ takes place to form $(\text{Q}^-\text{NH}^+)^*$ because of the instability of $(^-\text{QNH}^+)^*$ compared

Table 1. The Fluorescence Wavelengths and Kinetic Time Constants of Intermediate Species at S_1 in 6HQN Aqueous Solutions

| Intermediate | λ_{peak} (nm) | Kinetic Time Constant (ps) | | | | | |
|-------------------------|------------------------------|------------------------------|-----------------|---------------------|-------|-------------------|-------|
| | | Neutral H_2O | | 4-M HClO_4 | | 1-M NaOH | |
| | | Rise | Decay | Rise | Decay | Rise | Decay |
| HQN | 380 | Instant | 15 | Not-Formed | | Not-Formed | |
| HQN^+ | 440 | 15 | 40 | Instant | 960 | Not-Formed | |
| ^-QN | 450 | Not-Formed | | Not-Formed | | Instant | 15 |
| $^-\text{QNH}^+$ | 510 | 40 | 11 ^a | 960 | 26 | 15 | 48 |
| Q^-NH^+ | 560 | 30 | 570 | 26 | 890 | 48 | 710 |

^a Calculated from the decay time of $(^-\text{QNH}^+)^*$ and the rise time of $(\text{Q}^-\text{NH}^+)^*$.

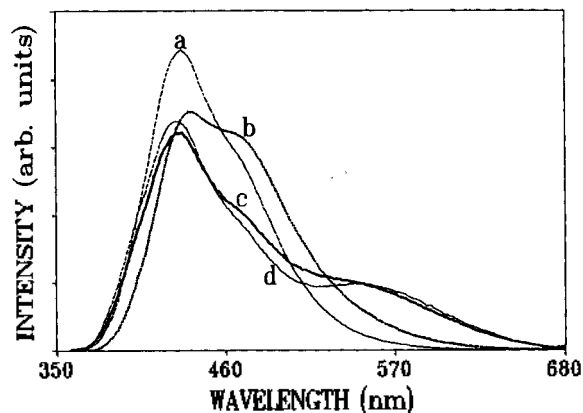


Figure 4. Area-normalized emission spectra, excited at 350 nm, of 0.1-mM 6HQN aqueous solutions where HClO_4 coexists as 11 (a), 7 (b), 3 (c) and 0.6 (d) M, respectively.

with $(\text{Q}^-\text{NH}^+)^*$ and reduces the electric dipole moment, the stabilization of $(\text{Q}^-\text{NH}^+)^*$ having a larger dipole moment may slow down the charge transfer process. The retardation by changing the solution from neutral to strongly acidic one can be easily understood since highly concentrated ionic species in strongly acidic solution stabilize the excited zwitterionic protropic species with a larger dipole. Even the slower electron rearrangement rate in 1-M NaOH solution than in 4-M HClO_4 solution can be explained by the reason that monatomic Na^+ and diatomic OH^- ions in NaOH solution have higher charge densities than polyatomic H_3O^+ and ClO_4^- ions in HClO_4 solution so that the ions in NaOH solution stabilize charges and charged species more efficiently.

Although the lifetimes of the excited Q^-NH^+ species in the studied three sample conditions of Table 1 are somewhat similar each other, the lifetime nevertheless increases with the increase of the ionic strength of solution. Note that the lifetime of the excited quinoid Q^-NH^+ in Table 1 is much shorter than the lifetime of 3 ns for the excited zwitterionic protropic species of 7-hydroxyquinoline.²⁹ This indicates that $(\text{Q}^-\text{NH}^+)^*$ is not so stable although it is reformed from the more unstable protropic zwitterionic $(\text{Q}^-\text{NH}^+)^*$ species by electron rearrangement and that $(\text{Q}^-\text{NH}^+)^*$ relaxes mainly by nonradiative processes. Internal conversion to S_0 is probably dominant among the processes and the conversion rate is known to decrease exponentially by the energy difference between S_1 and S_0 .⁴² The enlargement of $(\text{Q}^-\text{NH}^+)^*$ lifetime with the increment of the ionic strength indicates that Q^-NH^+ species should show hypsochromic blue shift with ionic strength increase although the S_1 states of hydroxyquinolines are known to have (π, π^*) character.³¹ Hypsochromic shift is usually not expected in (π, π^*) transition since it is possible when molecular dipole moment is larger in S_0 than in S_1 . Consider that Q^-NH^+ is stabler in S_1 than Q^-NH^+ with a relatively larger dipole moment while less stable in S_0 . As a consequence of this relative stability change, Q^-NH^+ is perturbed by Q^-NH^+ more in S_0 than in S_1 so that its dipole moment is larger in S_0 than in S_1 , justifying the observed hypsochromic shift and slowed relaxation rate of $(\text{Q}^-\text{NH}^+)^*$ with ionic strength increase.

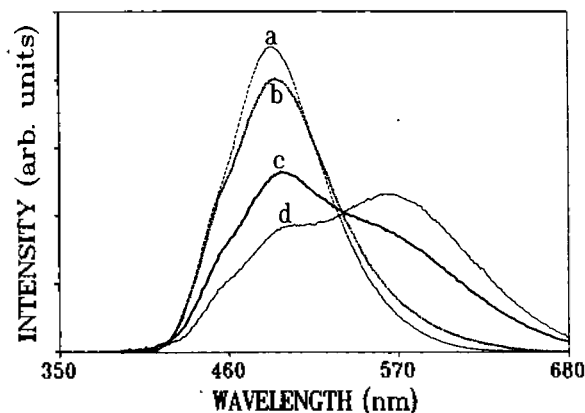


Figure 5. Area-normalized emission spectra, excited at 360 nm, of 0.2-mM 6HQN aqueous solutions where NaOH coexists as 11 (a), 7 (b), 2 (c) and 0.8 (d) M, respectively.

Knowing the formation and decay time constants of respective species in various sample conditions as discussed up to now and given in Table 1, we can describe rightly the meanings involved in the fluorescence spectra of aqueous 6HQN solutions with the various acidic and basic conditions of Figures 4 and 5 respectively. The emission band coming from excited Q^-NH^+ is now observable in the emission spectra of Figure 4 which were obtained by exciting HQNH^+ species in strongly acidic solutions with various HClO_4 concentrations. As $[\text{HClO}_4]$ decreases from 11 to 7 M so that deprotonation from the enol group becomes easier, the shoulder attributable to $(\text{Q}^-\text{NH}^+)^*$ fluorescence increases apparently. Then, a further decrease in $[\text{HClO}_4]$ must increase the deprotonation rate further. However, the shoulder as well as the absolute total fluorescence decreases with a further $[\text{HClO}_4]$ decrease as seen in the spectra (c) and (d). The reason why $(\text{Q}^-\text{NH}^+)^*$ fluorescence diminishes in spite of deprotonation rate acceleration with $[\text{HClO}_4]$ diminution is that $(\text{Q}^-\text{NH}^+)^*$ becomes more unstable with a lower ionic strength and transforms more rapidly into stabler $(\text{Q}^-\text{NH}^+)^*$ by electron rearrangement. Since the formation of $(\text{Q}^-\text{NH}^+)^*$ is much faster than its decay in the sample conditions of (c) and (d) and its decay speeds up with ionic strength decrease, the absolute intensity of $(\text{Q}^-\text{NH}^+)^*$ fluorescence as well as that of total fluorescence diminishes with $[\text{HClO}_4]$ decrement. It is quite interesting to examine the wavelength shifts in the blue region of the normal fluorescence with $[\text{HClO}_4]$ variations. $[\text{HClO}_4]$ attenuation from 11 to 7 M exhibits a red shift while its further attenuation to 3 and 0.6 M reveals a blue shift. These wavelength shifts suggest that the S_1 state of HQN species in these strongly acidic solutions has both characters of (n, π^*) and (π, π^*) as in Eq. (5)

$$\text{S}_1 = C_n(n, \pi^*) + C_\pi(\pi, \pi^*) \quad (5)$$

where C_n and C_π are the respective fractions of (n, π^*) and (π, π^*) contributions. Both (n, π^*) and (π, π^*) states are energetically very close and C_n becomes smaller with ionic strength reduction. It is well known that (n, π^*) transition shows hypsochromic shift while bathochromic shift is observed in (π, π^*) transition with ionic strength increase. (n, π^*) transition is prevailing and shifts largely to the red with

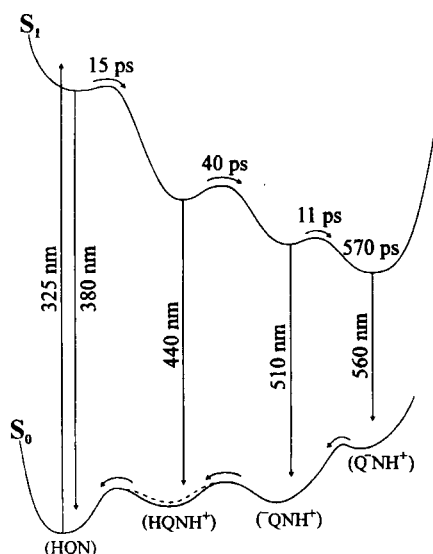


Figure 6. Schematic representation of proton transfers and subsequent electron rearrangement of aqueous 6HQN in the first excited singlet states. The wavelengths of peak absorption and fluorescence for 6HQN protropic species are indicated beside the respective vertical arrows. The relative position of the ground state of ${}^{-}\text{QN}$ is indicated by the dotted potential well just over the ground state of HQNH^+ .

$[\text{HClO}_4]$ decrease in the sample conditions of spectra (a) and (b) while (π, π^*) transition becomes dominant and shows a very slight blue shift with $[\text{HClO}_4]$ reduction at the low ionic strengths of spectra (c) and (d).

The emission spectra (a) and (b) in Figure 5 look like a single fluorescence band, mainly originating from the excited zwitterionic protropic $({}^{-}\text{QNH}^+)^*$ species which was asserted³² not to fluoresce. The kinetic time constants of the 1-M NaOH-dissolved sample in Table 1 suggest that $({}^{-}\text{QNH}^+)^*$ transformed immediately from $({}^{-}\text{QN})^*$ by imine protonation may stay long without intramolecular charge transfer in the strongly basic solutions of spectra (a) and (b). As $[\text{NaOH}]$ reduces further to 2 and 0.8 M, the charge transfer quickens and $({}^{-}\text{QNH}^+)^*$ fluorescence intensity gets smaller. As already described during the interpretation of Figure 4, the absolute intensity of $(\text{Q}^-\text{NH}^+)^*$ fluorescence as well as that of total fluorescence decreases with $[\text{NaOH}]$ reduction since the formation is much faster than its decay and its decay rate becomes higher with ionic strength reduction. Only the barely noticeable small shoulder can be observable near 450 nm for all the spectra of Figure 5, for excited state protonation to the nitrogen atom is extremely fast even at strongly basic conditions.

Important observations and our proposed mechanism for the photochemical and photophysical phenomena at S_1 states of neutral aqueous 6HQN solution are summarized in Figures 1 and 6. Protonation to the imine group from a hydrogen-bonded water molecule takes place first in 15 ps, generating protonated $(\text{HQNH}^+)^*$ as the reaction intermediate in the course of protropic tautomerization. $({}^{-}\text{QNH}^+)^*$ is then generated in 40 ps by the deprotonation from the enol group of $(\text{HQNH}^+)^*$ to a hydrogen-bonded water molecule, forming the protropic tautomer, $({}^{-}\text{QNH}^+)^*$ of normal species $(\text{HQN})^*$. Since $(40 \text{ ps})^{-1}$ corresponds to

38% of $(15 \text{ ps})^{-1}$, we should also observe $({}^{-}\text{QN})^*$ as a reaction intermediate during protropic tautomerization and $({}^{-}\text{QN})^*$ fluorescence should be about 38% of $(\text{HQNH}^+)^*$ fluorescence if enol deprotonation competes with imine protonation in $(\text{HQN})^*$ species. No observation of $({}^{-}\text{QN})^*$ fluorescence indicates that the enol deprotonation of $(\text{HQN})^*$ must be much slower than that of $(\text{HQNH}^+)^*$. We hypothesize that the faster deprotonation of $(\text{HQNH}^+)^*$ is owing to catalysis by the OH^- produced from the deprotonation of the hydrogen-bonded water to the N atom during the first protonation process, which obviously, within 40 ps, stays near the $(\text{HQNH}^+)^*$ produced together. The excited protropic tautomer $({}^{-}\text{QNH}^+)^*$ is unstable and immediately (11 ps) transformed into an excited quinoid form $(\text{Q}^-\text{NH}^+)^*$ by intramolecular charge transfer from the deprotonated oxygen atom to the positively charged iminium ring. $(\text{Q}^-\text{NH}^+)^*$ is the final photochemical product after consecutive proton and electron transfers in S_1 and relaxes to the ground state in 570 ps. Q^-NH^+ species shows a smaller dipole moment in S_1 than in S_0 and a hypsochromic shift with ionic strength increment although its S_1 state has (π, π^*) character.

Acknowledgment. We thank Dr. Dongho Kim and Dr. Nam Woong Song at the Korea Research Institute of Standards and Science for emission profile measurements. This work and publication cost were supported by the Korea Ministry of Education and the Research Institute of Molecular Science respectively.

References

- †. Also a member of the Center for Molecular Science, Taejon 305-701, Korea.
1. Turro, N. J. *Modern Molecular Photochemistry*; University Science Books: Mill Valley, California, 1991; p 228.
2. Klöpffer, W. *Adv. Photochem.* **1977**, *10*, 311.
3. Verdasco, G.; Martin, M. A.; del Castillo, B.; López-Alvarado, P. Menéndez, J. C. *Anal. Chim. Acta* **1995**, *303*, 73.
4. Cummings, S. D.; Eisenberg, R. *Inorg. Chem.* **1995**, *34*, 3396.
5. Linares, R. M.; González, A.; Ayala, J. H.; Afonso, A. M.; González, V. *Spectrochim. Acta Part A*, **1995**, *51*, 1691.
6. Park, H.-R.; Mayer, B.; Wolschann, P.; Köhler, G. *J. Phys. Chem.* **1994**, *98*, 6158.
7. Douhal, A.; Amat-Guerri, F.; Acuña, A. U. *J. Phys. Chem.* **1995**, *99*, 76.
8. Shafirovich, V. Y.; Courtney, S. H.; Ya, N.; Geacintov, N. E. *J. Am. Chem. Soc.* **1995**, *117*, 4920.
9. Hassoon, S.; Neckers, D. C. *J. Phys. Chem.* **1995**, *99*, 9416.
10. Hara, K.; Kometani, N.; Kajimoto, O. *J. Phys. Chem.* **1996**, *100*, 1488.
11. Mac, M.; Najbar, J.; Wirz, J. *Chem. Phys. Lett.* **1995**, *235*, 187.
12. Gao, M.; Hill, R. H. *J. Photochem. Photobiol. A: Chem.* **1996**, *97*, 73.
13. Niu, Y.; Christophy, E.; Pisano, P. J.; Zhang, Y.; Hossenlopp, J. M. *J. Am. Chem. Soc.* **1996**, *118*, 4181.
14. Castellan, A.; Grelier, S.; Kessab, L.; Nourmamode, A.;

- Hannachi, Y. *J. Chem. Soc., Perkin Trans. 2* **1996**, 1131.
15. Benjamin, I. *J. Chem. Phys.* **1995**, *103*, 2459.
 16. Karge, M.; Irrgang, K.-D.; Sellin, S.; Feinäugle, R.; Liu, B.; Eckert, H.-J.; Eichler, H. J.; Renger, G. *FEBS Lett.* **1996**, *378*, 140.
 17. Huppert, D.; Gutman, M.; Kaufmann, K. J. *Adv. Chem. Phys.* **1981**, *47*, 643.
 18. Chudoba, C.; Lutgen, S.; Jentsch, T.; Riedle, E.; Woerner, M.; Elsaesser, T. *Chem. Phys. Lett.* **1995**, *240*, 35.
 19. Syage, J. A. *J. Phys. Chem.* **1995**, *99*, 5772.
 20. Logunov, S. L.; El-Sayed, M. A.; Song, L.; Lanyi, J. K. *J. Phys. Chem.* **1996**, *100*, 2391.
 21. Brückner, V.; Feller, K.-H.; Grummt, U.-W. *Application Of Time-Resolved Optical Spectroscopy*; Elsevier Science: New York, 1990; p 61.
 22. Nijhawan, M.; Chauhan, R. S.; Kakkar, L. R. *Bull. Chem. Soc. Jpn.* **1995**, *68*, 2885.
 23. Djane, N.-K.; Malcus, F.; Martins, E.; Sawula, G.; Johansson, G. *Anal. Chim. Acta* **1995**, *316*, 305.
 24. Burrows, P. E.; Forrest, S. R. *Appl. Phys. Lett.* **1994**, *64*, 2285.
 25. Rompf, C.; Ammermann, D.; Kowalsky, W. *Mater. Sci. Technol.* **1995**, *11*, 845.
 26. Matsumura, M.; Akai, T.; Saito, M.; Kimura, T. *J. Appl. Phys.* **1996**, *79*, 264.
 27. Douhal, A.; Dabrio, J.; Sastre, R. *J. Phys. Chem.* **1996**, *100*, 149.
 28. Kim, T. G.; Lee, S.-I.; Jang, D.-J.; Kim, Y. *J. Phys. Chem.* **1995**, *99*, 12698.
 29. Lee, S.-I.; Jang, D.-J. *J. Phys. Chem.* **1995**, *99*, 7537.
 30. Lavin, A.; Collins, S. *J. Phys. Chem.* **1993**, *97*, 13615.
 31. Kang, W.-K.; Cho, S.-J.; Lee, M.; Kim, D.-H.; Ryoo, R.; Jung, K.-H.; Jang, D.-J. *Bull. Korean Chem. Soc.* **1992**, *13*, 140.
 32. Bardez, E.; Chatelain, A.; Larrey, B.; Valeur, B. *J. Phys. Chem.* **1994**, *98*, 2357.
 33. Laks, P. E.; Rettig, S. J.; Trotter, J. *Acta Cryst.* **1986**, *C 42*, 1799.
 34. Shah, K. J.; Coats, E. A. *J. Med. Chem.* **1977**, *20*, 1001.
 35. Chung, K. H.; Cho, K. Y.; Asami, Y.; Takahashi, N.; Yoshida, S. *Z. Naturforsch.* **1989**, *44c*, 609.
 36. Mason, S. F.; Philp, J.; Smith, B. E. *J. Chem. Soc. (A)* **1968**, 3051.
 37. Yoshinari, T.; Okada, H.; Yamada, A.; Uemura, D.; Oka, H.; Suda, H.; Okura, A. *Jpn. J. Cancer Res.* **1994**, *85*, 550.
 38. Konishi, M.; Ohkuma, H.; Sakai, F.; Tsuno, T.; Koshiyama, H.; Naito, T.; Kawaguchi, H. *J. Am. Chem. Soc.* **1981**, *103*, 1241.
 39. Held, A.; Plusquellic, D. F.; Tomer, J. L.; Pratt, D. W. *J. Phys. Chem.* **1991**, *95*, 2877.
 40. Leeaphon, M.; Rohl, K.; Thomas, R. J.; Fanwick, P. E.; Walton, R. A. *Inorg. Chem.* **1993**, *32*, 5562.
 41. Park, J.; Kang, W.-K.; Ryoo, R.; Jung, K.-H.; Jang, D.-J. *J. Photochem. Photobiol. A: Chem.* **1994**, *80*, 333.
 42. Siebrand, W. *J. Chem. Phys.* **1967**, *47*, 2411.

Nucleophilic Substitution Reactions of 1- and 2-Naphthylmethyl Arenesulfonates with Anilines

Hyuck Keun Oh, Se Jeong Song, Chul Ho Shin, and Ikchoon Lee*

Department of Chemistry, Chonbuk National University, Chonju 560-756, Korea

**Department of Chemistry, Inha University, Incheon 402-751, Korea*

Received October 10, 1996

Kinetic studies are carried out on the reactions of 1- and 2-naphthylmethyl arenesulfonates with anilines in acetonitrile at 25.0 °C. The rates are faster for the 2-naphthylmethyl series than for the corresponding 1-naphthylmethyl series suggesting that there is a greater stabilization of positive charge development in the TS at the arylmethyl reaction center carbon for the former. The sign and magnitude of ρ_{XZ} ($= -0.12$) are similar to those of the benzylic series. Thus, benzyl, 1- and 2-naphthylmethyl derivatives belong to a class of compounds which react with aniline nucleophiles through a relatively loose S_N2 TS. Kinetic secondary deuterium isotope effects indicated that a stronger nucleophile and nucleofuge lead to a later TS as the definition of ρ_{XZ} requires.

Introduction

The sign and magnitude of cross-interaction constant ρ_{XZ} , Eqs. 1, are shown to have important mechanistic significances for organic reactions in solution.¹ In these expressions, X and Z denote substituents in the nucleophile and leaving group respectively. The simple second-order

equation 1a is arrived at by a Taylor series expansion of $\log k_{XZ}$ around $\rho_X = \rho_Z = 0$ and neglecting pure second- and higher-order terms.¹

$$\log(k_{XZ}/k_{HH}) = \rho_X \sigma_X + \rho_Z \sigma_Z + \rho_{XZ} \sigma_X \sigma_Z \quad (1a)$$

$$\rho_{XZ} = \frac{\partial^2 \log k_{XZ}}{\partial \sigma_X \partial \sigma_Z} = \frac{\partial \rho_Z}{\partial \sigma_X} = \frac{\partial \rho_X}{\partial \sigma_Z} \quad (1b)$$